Novel Class of Chalcone Oxime Ethers as Potent Monoamine Oxidase-B and Acetylcholinesterase Inhibitors

Jong Min Oh [1], T. M. Rangarajan [2,*], Reeta Chaudhary [3,4], Rishi Pal Singh [2], Manjula Singh [5], Raj Pal Singh [3], Anna Rita Tondo [6], Nicola Gambacorta [6], Orazio Nicolotti [6], Bijo Mathew [7,*] and Hoon Kim [1,*]

[1] Department of Pharmacy, and Research Institute of Life Pharmaceutical Sciences, Sunchon National University, Suncheon 57922, Korea; ddazzo005@naver.com

[2] Department of Chemistry, Sri Venketeswara College, University of Delhi, New Delhi-110021, India; rpsingh54@gmail.com

[3] Centre for Fire, Explosive and Environment Saftey, DRDO, Delhi-110054, India; chaudhary.reeta90@gmail.com (R.C.); rajcfees@gmail.com (R.P.S.)

[4] Department of Chemistry, University of Dehli, Dehli-110007, India

[5] Department of Chemistry, Shivaji College, University of Delhi, New Delhi-110027, India; manjulasingh56@gmail.com

[6] Dipartimento di Farmacia—Scienze del Farmaco, Università degli Studi di Bari "Aldo Moro", via E. Orabona, 4, I-70125 Bari, Italy; annarita.tondo@gmail.com (A.R.T.); nicola.gambacorta1@uniba.it (N.G.); onicolotti@gmail.com (O.N.)

[7] Division of Drug Design and Medicinal Chemistry Research Lab, Department of Pharmaceutical Chemistry, Ahalia School of Pharmacy, Palakkad-678557, Kerala, India

* Correspondence: rangarajan93150@gmail.com (T.M.R.); bijo.mathew@ahalia.ac.in (B.M.); hoon@sunchon.ac.kr (H.K.)

Abstract: Previously synthesized novel chalcone oxime ethers (COEs) were evaluated for inhibitory activities against monoamine oxidases (MAOs) and acetylcholinesterase (AChE). Twenty-two of the 24 COEs synthesized, except **COE-17** and **COE-24**, had potent and/or significant selective inhibitory effects on MAO-B. **COE-6** potently inhibited MAO-B with an IC_{50} value of 0.018 μM, which was 105, 2.3, and 1.1 times more potent than clorgyline, lazabemide, and pargyline (reference drugs), respectively. **COE-7**, and **COE-22** were also active against MAO-B, both had an IC_{50} value of 0.028 μM, which was 67 and 1.5 times lower than those of clorgyline and lazabemide, respectively. Most of the COEs exhibited weak inhibitory effects on MAO-A and AChE. **COE-13** most potently inhibited MAO-A (IC_{50} = 0.88 μM) and also significantly inhibited MAO-B (IC_{50} = 0.13 μM), and it could be considered as a potential nonselective MAO inhibitor. **COE-19** and **COE-22** inhibited AChE with IC_{50} values of 5.35 and 4.39 μM, respectively. The selectivity index (SI) of **COE-22** for MAO-B was higher than that of **COE-6** (SI = 778.6 vs. 222.2), but the IC_{50} value (0.028 μM) was slightly lower than that of **COE-6** (0.018 μM). In reversibility experiments, inhibitions of MAO-B by **COE-6** and **COE-22** were recovered to the levels of reference reversible inhibitors and both competitively inhibited MAO-B, with K_i values of 0.0075 and 0.010 μM, respectively. Our results show that **COE-6** and **COE-22** are potent, selective MAO-B inhibitors, and **COE-22** is a candidate of dual-targeting molecule for MAO-B and AChE.

Keywords: monoamine oxidase; acetylcholinesterase; chalcones; oximes; kinetics; reversibility

1. Introduction

Alzheimer's disease (AD) is one of the greatest concerns confronting the medical community, and is the fourth leading cause of neurodegenerative disease-related death. Furthermore, AD has been predicted to affect 100 million patients within 30 years [1]. AD accounts for 70% of all reported cases of dementia, being characterized by cholinergic functional decline, β-amyloid oligomer formation, and the dysregulations of other cellular processes [2]. Over past years, many efforts have been made to identify the key biochemical events responsible for AD. However, AD is a multifactorial disease and, thus, its management requires the simultaneous modulations of multiple targets [3]. Based on greater understanding of the disease, recent research efforts have increasingly focused on multitarget-drugs that simultaneously bias different biological targets [4].

This novel approach is viewed optimistically, and hybridizations of the pharmacophore subunits of bioactive molecules have already resulted in the identification of multifunctional drugs [5] and, as a result, synthetic drugs, like donepezil, rivastigmine, and tacrine, have been used as structural models for molecular hybridization experiments (Figure 1) [6]. Tacrine was the first cholinesterase (ChE) inhibitor that was approved by the FDA for the treatment of AD. However, the use of tacrine is limited by its side-effects and, thus, searches for more compatible and potent tacrine derivatives continue [7].
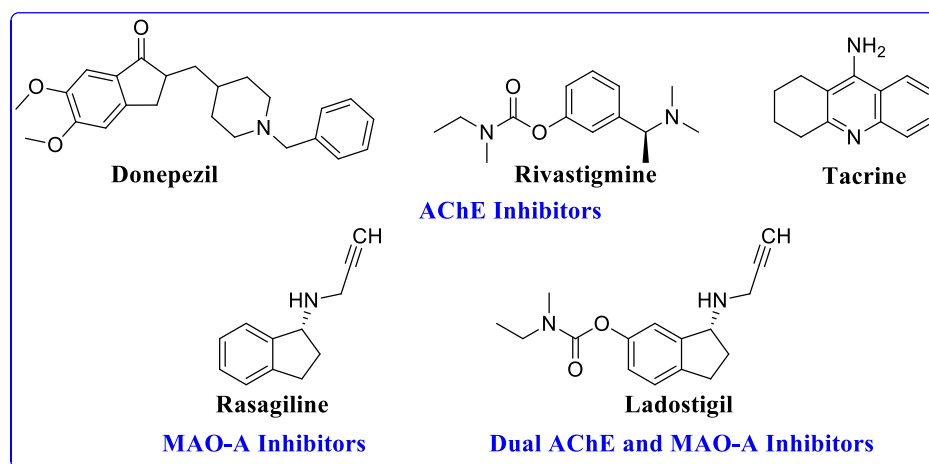

Figure 1. Structures of some FDA approved acetylcholinesterase (AChE) and MAO-A inhibitors.

On the other hand, monoamine oxidase (MAO)-A is primarily targeted for the treatment of depression and anxiety, whereas MAO-B is targeted for AD and Parkinson's disease, based on their specificity, which is, MAO-A prefers serotonin, and MAO-B prefers phenylethylamine and benzylamine [8]. Rasagiline is a MAO inhibitor, and its neuroprotective activity has been attributed to the presence of a propargyl amine moiety, which suppresses the overexpression of Bax protein in AD [9].

The complexity of AD militates against the use of consolidated mono-therapies and supports the notion that dual MAO and acetylcholinesterase (AChE)-inhibitory activities are likely to have better therapeutic effects in AD [10]. Ladostigil is an example of such multi-functional drugs, as it possesses the neuroprotective effects of rasagiline and ChE inhibitory activity (Figure 1) [11]. Notably, most drugs used to treat AD patients in palliative care settings are ChE inhibitors with some multifunctional activity. Furthermore, many studies have shown that MAO inhibitors have attracted considerable research interest in the context of halting or retarding the progression of AD [4].

Chalcones are versatile scaffolds and they are widely distributed in edible plants. Several attempts have been made to synthesize novel biologically active chalcone derivatives due to their wide-ranging biological activities [12–16]. Over recent decades, the MAO-B inhibitory activities of chalcone derivatives have progressively appreciated [17], and many studies have reinforced the

association between chalcone derivatives and potent MAO-B inhibition [18–35]. Recently, our group reported that ethoxy and ethyl acetohydroxamate (Figure 2) functionalities on chalcone phenyl groups confer significant MAO-B and AChE inhibitory effects [36,37].
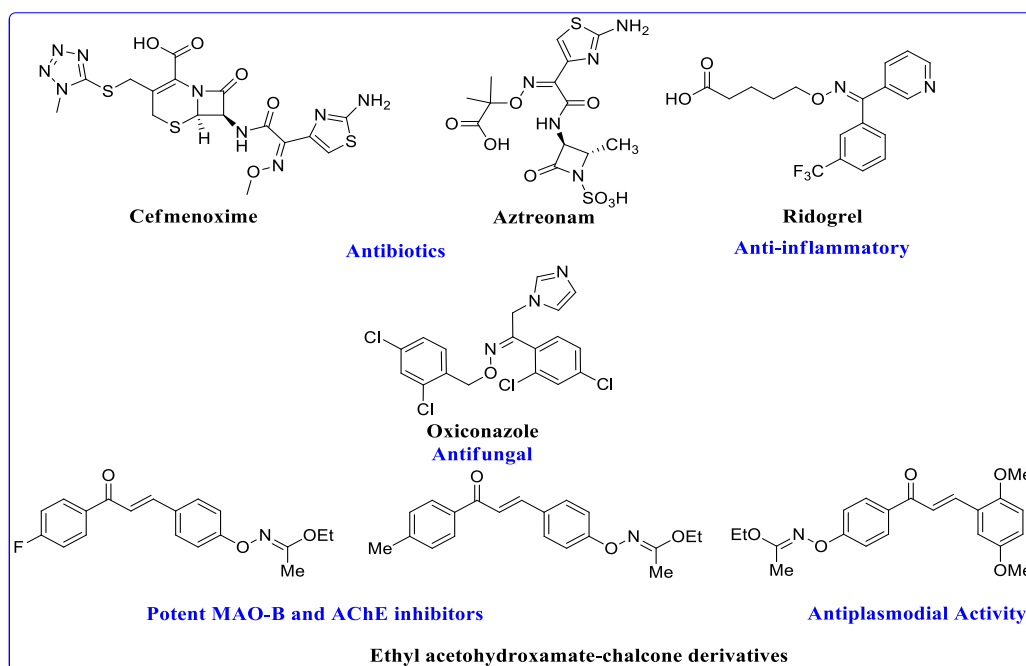

Figure 2. Structures of various biologically active compounds containing oxime moieties.

The oxime ethers are among the most important structural pharmaceutical motifs, for example, they have been associated with transthyretin amyloid fibril formation [38], antibiotic (Cefmenoxime [39], Aztreonam [40], Roxithromycin [41]), anti-inflammatory (Ridogrel) [42], antifungal (Oxiconazole) [43] (Figure 2), and neuroleptic activities [44]. We considered manipulating the ethyl acetohydroxamate functionality in ethyl acetohydroxamate chalcones by introducing an oxime to produce a range of novel chalcone oxime ethers (COEs) with the objective of synthesizing drugs with MAO and AChE inhibitory effects for the treatment of AD since oxime ethers have numerous biological properties and ethyl acetohydroxamate chalcones have significant MAO-B and AChE inhibitory [37] (Figure 2) and antiplasmodial [45] effects. Recently, we used Pd-catalyzed C-O cross-coupling reactions between bromo-chalcones and aldoximes [46], or ketoximes [47] in order to synthezise the chalcones, as shown in Scheme 1.
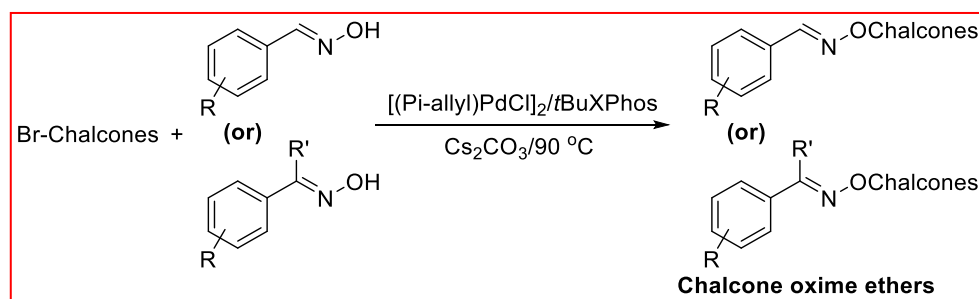

Scheme 1. Pd-catalyzed C-O cross-coupling reactions of bromo-chalcones with oximes.

Herein, we report the abilities of our previously synthesized chalcone ketoxime ethers to inhibit human MAOs (hMAOs) and AChE, kinetics, reversibility, and docking studies.

2. Results and Discussion

2.1. Synthesis of COEs

Pd-catalyzed C-O cross-coupling was used to produce 24 COEs by reacting activated aryl bromides, ketoximes, and chalcone oximes together, as shown in Scheme 2, and previously described [47].
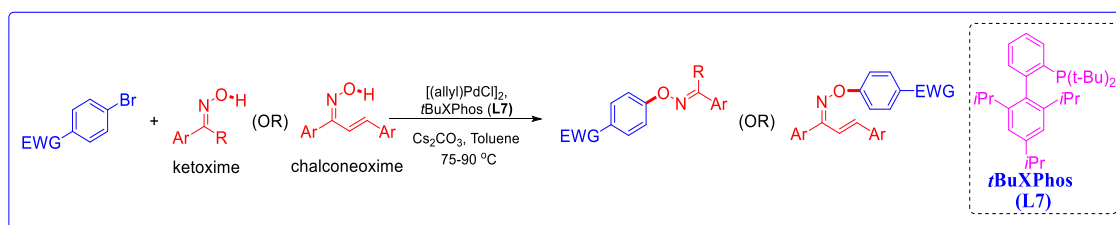
Scheme 2. Pd-catalyzed C-O coupling of activated aryl bromides with ketoximes and chalcone oximes.

The activated aryl bromides included aryl bromides bearing electron-withdrawing groups at the 4-position and bromo-chalcones. Screening phosphine ligands, Pd-catalyst, and solvents was utilized to optimize the method.

2.2. Inhibitory Activities against MAO-A, MAO-B and AChE

The MAO-A, MAO-B, and AChE inhibitory activities of 24 synthesized COEs were evaluated while using toloxatone, lazabemide, clorgyline, pargyline, and tacrine as reference molecules (Table 1). The synthesized COEs were of two structural categories, that is, chalcone ketoxime or chalcone-chalcone oxime hybrids. Nineteen of the 24 COEs showed residual MAO-B activities of <50% at 1.0 μM and potently inhibited MAO-B with IC_{50} values of <1.0 μM (Table 1). Eight of the 19 showed significant MAO-B inhibitory activities with IC_{50} values of <0.1 μM, and compound **COE-6** most potently inhibited MAO-B (IC_{50} = 0.018 μM), and **COE-7** and **COE-22** had equally significant MAO-B inhibitory activity (both IC_{50} = 0.028 μM). Interestingly, **COE-6** and pargyline had an identical IC_{50} value (0.020 μM) and they were 2.33 and 105.6 times more potent than lazabemide and clorgyline, respectively, and **COE-6** was more potent than other chalcone derivatives, (2E)-1-(4-ethoxyphenyl)-3-(4-fluorophenyl) prop-2-en-1-one (**E7,** IC_{50} = 0.053 μM) [36], and ethyl (1E)-N-{4-[(1E)-3-(4-fluorophenyl)-3-oxoprop-1-en-1-yl]phenoxy}ethanimidate (**L3,** IC_{50} = 0.053 μM) [37]. Similarly, **COE-7** and **COE-22** were 1.5 and 68 times more potent than lazabemide and clorgyline, respectively.

Twenty three of the 24 COEs showed residual MAO-A activities of >60% at 1.0 μM, but only **COE-13** had a residual activity of <50% at 1.0 μM (Table 1). Twenty-three of the COEs screened relatively weakly inhibited MAO-A (IC_{50} > 4.0 μM). **COE-13** had an IC_{50} value of 0.88 μM and it was 1.1 and 2.8 times more potent than toloxatone (IC_{50} = 0.99 μM) and pargyline (IC_{50} = 2.43 μM), respectively. **COE-13** also significantly inhibited MAO-B (IC_{50} = 0.13 μM) and, thus, had a low selectivity index (SI) of 6.8. Twenty two of the 24 COEs inhibited MAO-B more than MAO-A, as was reflected by SI values (defined as the ratio of the IC_{50} values of MAO-A to MAO-B). Of the 24 COEs, only **COE-6, COE-7, COE-8, COE-21**, and **COE-22**, had high SI values. Compound **COE-8** (IC_{50} = 0.042 μM) had the lowest SI (182.9), and the most potent MAO-B inhibitor **COE-6** (IC_{50} = 0.018 μM) had the second lowest (222.2). The next most potent MAO-B inhibitors **COE-7** and **COE-22** (both had an IC_{50} of 0.028 μM) had SI values of 392.9 and 778.6, respectively, and **COE-21** (IC_{50} = 0.036 μM) had the second highest SI (441.7). This result shows that the chalcone-chalcone oxime hybrids tend to inhibit MAO-B more selectively than chalcone ketoxime hybrids.

AChE inhibition studies showed that only six compounds, **COE-5, COE-9, COE-10, COE-19, COE-21**, and **COE-22**, had AChE residual activities of <50% at 10 μM with IC_{50} values of 7.06, 8.39, 9.42, 5.35, 9.65, and 4.39 μM, respectively. However, AChE inhibitions by these compounds were approximately 22 times less than that of the reference tacrine. **COE-22** most potently inhibited AChE

and also inhibited MAO-B well and it had the highest SI value, which suggest its possible use for the dual-targeting of MAO-B and AChE.

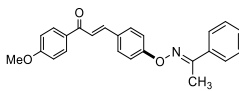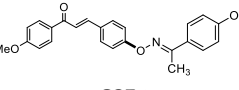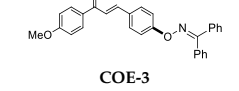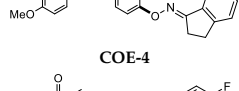**Table 1.** Inhibitions of recombinant human MAO-A, MAO-B, and AChE by chalcone oxime ethers[a].
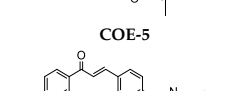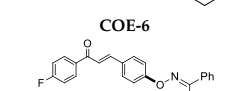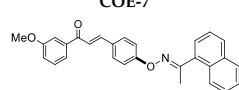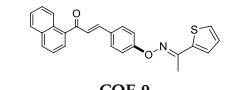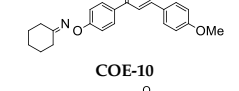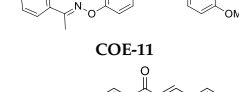
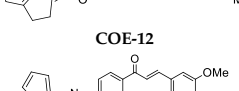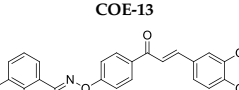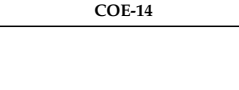| Chalcone Oxime Ethers (COEs)	Residual Activity (%)			IC$_{50}$ (µM)			
	MAO-A (1.0 µM)	MAO-B (1.0 µM)	AChE (10 µM)	MAO-A	MAO-B	AChE	SI[b]
Chalcone-ketoxime ethers							
COE-1	94.4 ± 2.99	29.9 ± 5.25	77.6 ± 2.64	>10	0.28 ± 0.041	>40	>35.7
COE-2	69.9 ± 0.51	27.6 ± 2.44	66.5 ± 3.36	>10	0.26 ± 0.055	15.2 ± 0.55	>38.5
COE-3	87.3 ± 1.00	21.6 ± 4.88	77.1 ± 0.66	>10	0.048 ± 0.021	>40	>208.3
COE-4	83.7 ± 1.54	4.31 ± 1.22	62.1 ± 1.51	19.3 ± 0.21	0.059 ± 0.012	>40	32.7
COE-5	95.1 ± 2.68	57.5 ± 7.01	46.5 ± 0.71	>10	1.12 ± 0.10	7.06 ± 1.50	>8.9
COE-6	76.8 ± 3.98	−1.06 ± 1.84	79.4 ± 3.97	4.00 ± 0.021	0.018 ± 0.0020	>40	222.2
COE-7	91.7 ± 6.43	2.48 ± 0.15	76.2 ± 1.02	11.0 ± 1.22	0.028 ± 0.0016	>40	392.9
COE-8	68.6 ± 2.74	10.5 ± 0.21	70.7 ± 3.26	7.68 ± 0.34	0.042 ± 0.021	>40	182.9
COE-9	71.4 ± 0.51	9.91 ± 1.83	46.7 ± 4.27	7.64 ± 0.16	0.037 ± 0.0057	8.39 ± 2.14	20.6
COE-10	67.1 ± 2.02	21.6 ± 1.22	47.6 ± 0.93	>10	0.21 ± 0.010	9.42 ± 0.031	>47.6
COE-11	86.0 ± 6.58	68.5 ± 1.83	87.2 ± 0.47	>10	1.82 ± 0.022	>40	>5.5
COE-12	95.7 ± 2.02	40.5 ± 0.10	72.0 ± 1.95	>10	0.27 ± 0.056	>40	>37.0
COE-13	46.2 ± 1.07	31.9 ± 9.75	57.6 ± 1.96	0.88 ± 0.030	0.13 ± 0.0069	>40	6.8
COE-14	91.1 ± 3.84	63.7 ± 1.39	62.2 ± 4.19	>10	1.58 ± 0.031	13.2 ± 0.84	>6.3
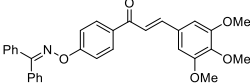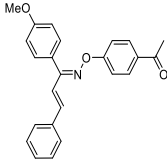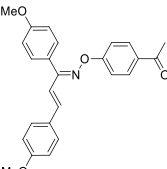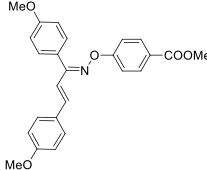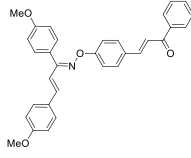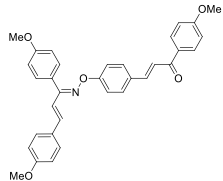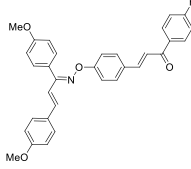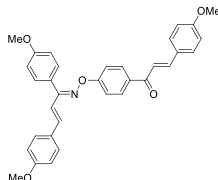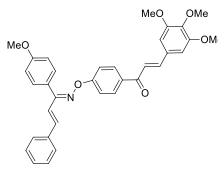
Table 1. *Cont.*

Chalcone Oxime Ethers (COEs)	Residual Activity (%)			IC$_{50}$ (μM)			
	MAO-A (1.0 μM)	MAO-B (1.0 μM)	AChE (10 μM)	MAO-A	MAO-B	AChE	SI[b]
COE-15	95.0 ± 3.03	36.9 ± 9.49	56.9 ± 1.40	>10	0.95 ± 0.029	>40	>10.5
Aryl chalcone oxime ethers COE-16	93.4 ± 3.44	97.8 ± 0.08	77.3 ± 6.62	>10	>10	>40	-
COE-17	80.9 ± 2.01	17.6 ± 2.77	80.3 ± 1.39	>10	0.72 ± 0.015	>40	>13.9
COE-18	88.1 ± 0.99	33.3 ± 0.52	58.3 ± 5.30	>10	0.85 ± 0.12	10.6 ± 0.26	>11.8
Chalcone-chalconeoxime ethers COE-19	85.3 ± 0.99	19.2 ± 3.06	39.0 ± 0.45	>10	0.32 ± 0.015	5.35 ± 0.68	>31.3
COE-20	89.7 ± 4.51	21.0 ± 0.42	60.6 ± 5.74	>10	0.35 ± 0.011	11.2 ± 1.33	>28.6
COE-21	85.8 ± 1.47	−2.19 ± 0.08	49.4 ± 2.90	15.9 ± 0.59	0.036 ± 0.0019	9.65 ± 1.20	441.7
COE-22	81.8 ± 0.99	5.47 ± 0.21	35.7 ± 0.64	21.8 ± 1.55	0.028 ± 0.0042	4.39 ± 2.68	778.6

Table 1. *Cont.*

Chalcone Oxime Ethers (COEs)	Residual Activity (%)			IC$_{50}$ (μM)			
	MAO-A (1.0 μM)	MAO-B (1.0 μM)	AChE (10 μM)	MAO-A	MAO-B	AChE	SI^b
COE-23	85.1 ± 4.01	25.8 ± 4.78	57.3 ± 1.34	>10	0.15 ± 0.021	9.16 ± 0.021	>66.7
COE-24	88.9 ± 0.98	87.4 ± 2.81	72.5 ± 2.91	>10	>10	>40	-
Toloxatone	-	-	-	0.99 ± 0.080	-	-	
Lazabemide	-	-	-	-	0.042 ± 0.0028	-	
Clorgyline	-	-	-	0.0046 ± 0.00055	1.90 ± 0.78	-	
Pargyline	-	-	-	2.43 ± 0.17	0.020 ± 0.00071	-	
Tacrine	-	-	-	-	-	0.20 ± 0.019	

^{a} Results are expressed as the means ± standard errors of duplicate experiments. ^{b} SI values are expressed as MAO-A vs. MAO-B ratios. Results for reference compounds were determined after preincubation with enzymes for 30 min.

2.3. SARs for Inhibition Studies

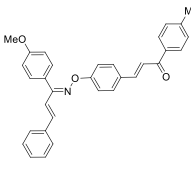Twenty two of 24 COEs included in the present study were selective MAO-B inhibitors (Table 1). The activity results showed that the activity of the COEs depended on the structures and substituents of oximes and chalcones. For example, in compounds **COE-1** to **COE-4**, structures and the substituent (-OMe) on the chalcone moiety were the same and substituents and structures of oximes differed. The substituents on acetophenone oxime of the chalcone moieties of **COE-1** and **COE-2** had no meaningful influence on MAO-B inhibition, whereas the conversion of acetophenone oxime (**COE-1**) to benzophenone oxime (**COE-3**) and 1-indanone oxime (**COE-4**) on the chalcone moiety increased MAO-B inhibition by 5.8 and 4.7 times, respectively. Similarly, the removal of –OMe from chalcone and introduction of a F at the 4-position of acetophenone oxime of **COE-1** greatly reduced the MAO-B inhibitory activity of **COE-5** (IC$_{50}$ = 1.12 μM) four-fold. Introduction of F in place of the -OMe group in chalcone moiety of **COE-3** structure (IC$_{50}$ = 0.048 μM) enhanced the MAO-B inhibitory activity of the compound **COE-7** (IC$_{50}$ = 0.028 μM) 1.7-fold, which suggested that the presence of F increases MAO-B inhibitory activity more than –OMe group, similar to other chalcone derivatives containing F [48]. Similarly, replacement of the benzophenone oxime of **COE-7** with cyclohexanone oxime in **COE-6** (IC$_{50}$ = 0.028 μM) enhanced MAO-B inhibitory activity by 1.5-fold. The presence of a F in acetophenone oxime in **COE-5** (IC$_{50}$ = 1.12 μM) and in **COE-11** (IC$_{50}$ = 1.82 μM) reduced MAO-B inhibition, irrespective of the substituents on or the position of oxime in chalcone structure. The position of the 1-acetonaphthone oxime in the chalcone structures of **COE-8** (IC$_{50}$ = 0.042 μM) and **COE-14** (IC$_{50}$ = 1.58 μM) also reduced MAO-B inhibitory activity. Similarly, the position of benzophenone oxime in the chalcone structures of **COE-3** (IC$_{50}$ = 0.048 μM) and **COE-15** (IC$_{50}$ = 0.95 μM) significantly altered MAO-B inhibitory activity. As a result, different ketoxime structures in the benzaldehyde portion of the chalcone structure had significantly greater MAO-B inhibitory activities than ketoxime structures in the acetophenone portion of chalcones. Our SAR study suggested that active oxime groups (e.g., benzophenone oxime, cyclohexanone oxime, acetothiophene oxime, and 1-acetonaphthone oxime) on benzaldehyde portions of chalcones and altering substituents and the structure on the acetophenones portion of chalcones provide a means of enhancing MAO-B inhibitory activities.

Of the three *O*-aryl chalcone oximes (**COE-16**, **COE-17**, and **COE-18**), two compounds, **COE-17** and **COE-18**, showed significantly higher MAO-B inhibitory activities (IC_{50} = 0.72 and 0.85 μM, respectively) than **COE-16** (IC_{50} > 10 μM). This result implies that the presence of two -OMe groups in the chalcone oxime structure greatly enhances MAO-B inhibition as compared with single -OMe group. Moreover, replacing the *O*-aryl group with an *O*-chalcone group (viz. **COE-19** to **COE-23)** improved the MAO-B inhibitory activity. In the dimethoxy chalcone oxime series, a F in the acetophenone portion of the chalcone, **COE-22**, resulted in excellent MAO-B inhibitory activity (IC_{50} = 0.028 μM), as compared with unsubstituted (-H), **COE-19** and –OMe substituted **COE-20**. The single -OMe substituted chalcone oxime with -Me group in the acetophenone portion of the chalcone moiety of **COE-21** also showed significant difference in MAO-B inhibitory activity (IC_{50} = 0.036 μM). This result suggests that electronegative groups enhance MAO-B inhibitory activity. The acetophenone portion of chalcone containing the -OMe group in **COE-20** significantly increased MAO-B inhibitory activity, when compared to the benzaldehyde portion containing the same group in **COE-23** (IC_{50} = 0.35 vs. 0.15 μM). These SAR studies afford great scopes of opportunity to synthesize more potent chalcone-chalcone oxime hybrid molecules, i.e., COEs.

No SAR study could be performed with respect to MAO-A inhibitory activity. Only one compound, **COE-13**, showed significant MAO-A inhibitory activity with an IC_{50} value of 0.88 μM, which in itself suggested that the presence of an acetothiophene oxime group in the acetophenone portion might enhance the MAO-A inhibitory activity. Interestingly, **COE-13** also inhibited MAO-A and MAO-B.

Similarly, only compound **COE-22**, a chalcone-chalcone oxime ether with a –F substituent, inhibited AChE (IC_{50} = 4.39 μM). Thus, **COE-22** may be considered a MAO-B and AChE dual inhibitor for the treatment of neurodegenerative diseases.

2.4. Kinetics of MAO-B Inhibitions

Kinetic studies were performed on MAO-B inhibition by **COE-6** and **COE-22**. Lineweaver–Burk plots and secondary plots showed that **COE-6** and **COE-22** competitively inhibited MAO-B (Figure 3A,C) with K_i values of 0.0075 ± 0.00067 and 0.010 ± 0.0035 μM, respectively (Figure 3B,D). These results suggest that **COE-6** and **COE-22** are potent, selective, and competitive inhibitors of MAO-B.

2.5. Reversibility Studies

Reversibility studies were conducted on MAO-B inhibition by **COE-6** and **COE-22**. In these experiments, inhibitions of MAO-B by **COE-6** and **COE-22** were recovered from 19.7 (A_U) to 81.1% (A_D) and from 22.6 (A_U) to 86.8% (A_D), respectively (Figure 4), and these values were similar to those of the reversible reference inhibitor lazabemide (from 2.4 to 76.4%). However, inhibition by the irreversible reference inhibitor pargyline was only slightly recovered (from 3.7 to 10.4%). These experiments showed that inhibitions of MAO-B by **COE-6** and **COE-22** were recovered to the reversible reference level, which suggested that both are reversible inhibitors.

2.6. Computational Studies

Computational analyses were performed using QM-polarized docking and MM-GBSA calculations in order to investigate the binding modes of **COE-6** and **COE-22** towards MAO-A and MAO-B and with the purpose of clarifying the MAO-B selectivity of the two compounds. Table 2 reports calculated docking scores and the Δ*G* binding values of the two compounds against MAO-A and MAO-B. In agreement with in vitro IC_{50} values, **COE-22** showed a better docking and MMGBSA scores for MAO-B compared to MAO-A. Conversely, **COE-6** did not show a significant gap in the docking score values between MAO-B and MAO-A.

Compound **COE-22** interacts with MAO-A and MAO-B with different binding modes (Figure 5). The residues of MAO-A involved in **COE-22** binding are Tyr62 and Lys218, which establish π and cation-π interactions, respectively, with the *para*-fluorine phenyl ring, Lys341, which engages a hydrogen bond with the carbonyl oxygen atom of the chalcone portion of **COE-22**, and Lys316, which forms a

cation-π interaction with the *para*-methoxy phenyl ring, as shown on panel (a) of Figure 5. Notably, the distance between the *para*-fluorine phenyl ring and aromatic rings of the flavin adenine dinucleotide (FAD) molecule is ~11 Å. On the other hand, as shown on panel (b) of Figure 5, the residues of MAO-B involved in **COE-22** binding are similar to those hypothesized in previous studies [25], whereby the *para*-fluorine phenyl ring of **COE-22** is trapped within an aromatic cage made up of FAD, Tyr398, and Tyr435. Furthermore, the *para*-fluorine phenyl ring, the *para*-methoxy styryl, and the chalcone aromatic ring establish π−π interactions with Tyr398, Trp119, and Tyr236 (MAO-B selective residue), respectively. In addition, the carbonyl oxygen of the chalcone scaffold of **COE-22** forms a hydrogen bond with the thiol group of Cys172.

Figure 3. *Cont.*

(C)

(D)
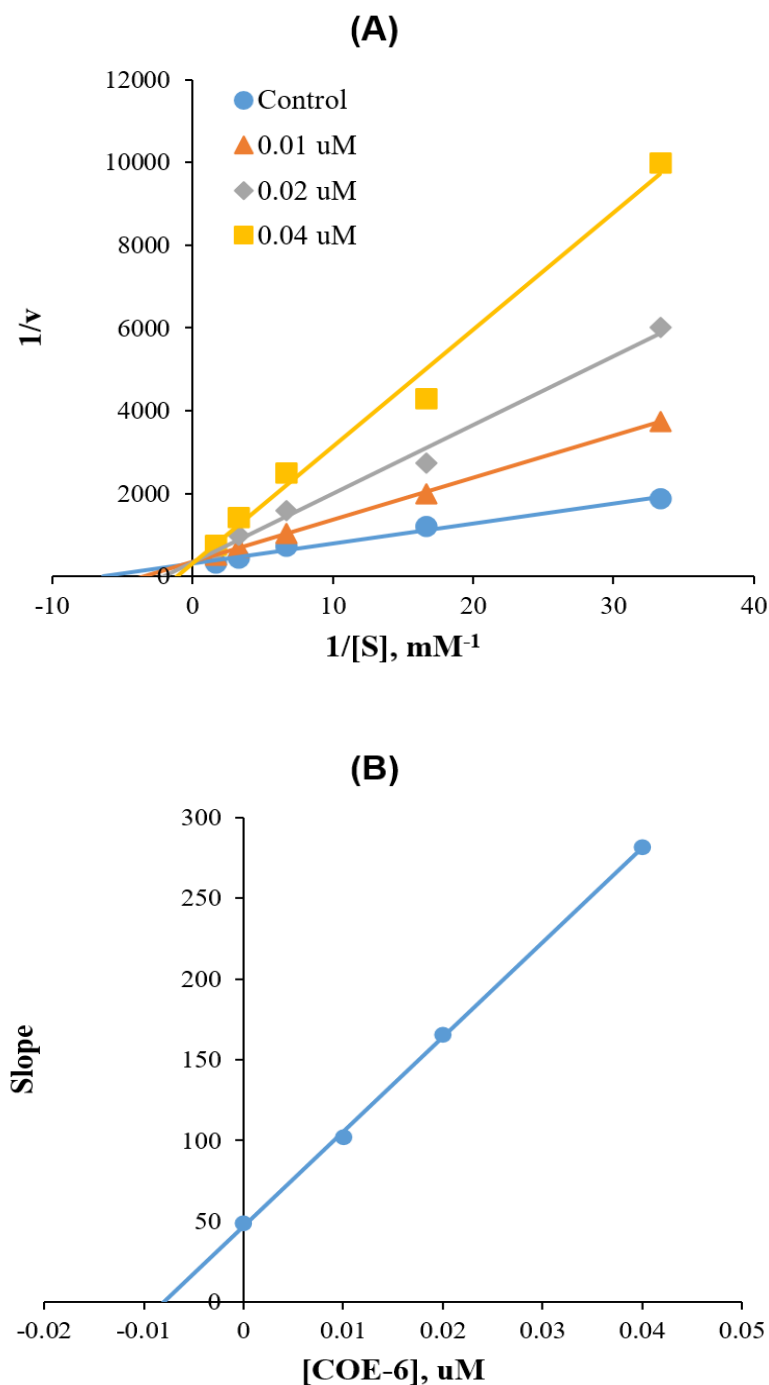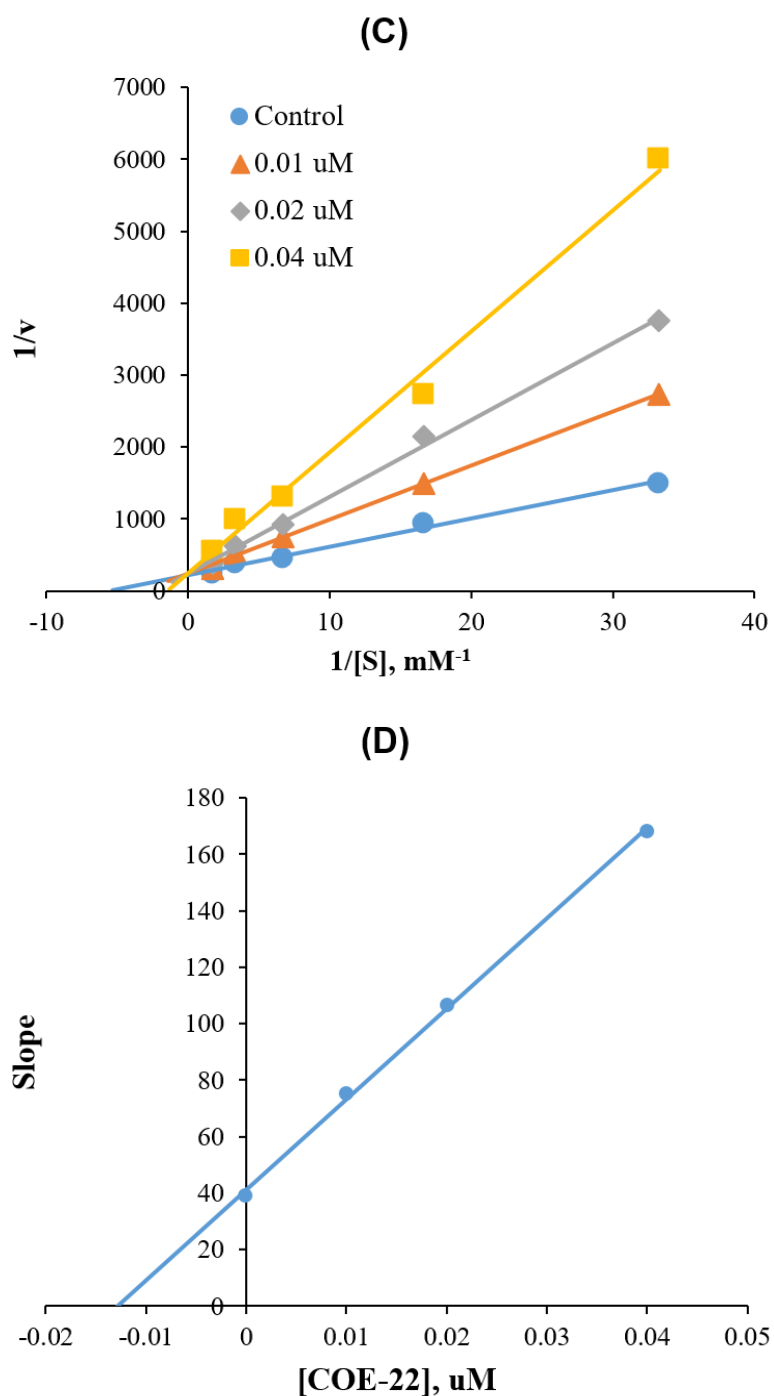
Figure 3. Lineweaver–Burk plots for MAO-B inhibition by **COE-6** (**A**) and **COE-22** (**C**), and their respective secondary plots (**B,D**) of slopes vs. inhibitor concentrations.

Table 2. Docking scores and ΔG binding values of lead compounds with MAO-A and MAO-B.

Compound	Docking Score (kcal/mol)		$\Delta G_{binding}$ (kcal/mol)	
	MAO-A	MAO-B	MAO-A	MAO-B
COE-6	−10.128	−11.728	−58.64	−82.65
COE-22	−7.785	−13.452	−60.57	−87.94
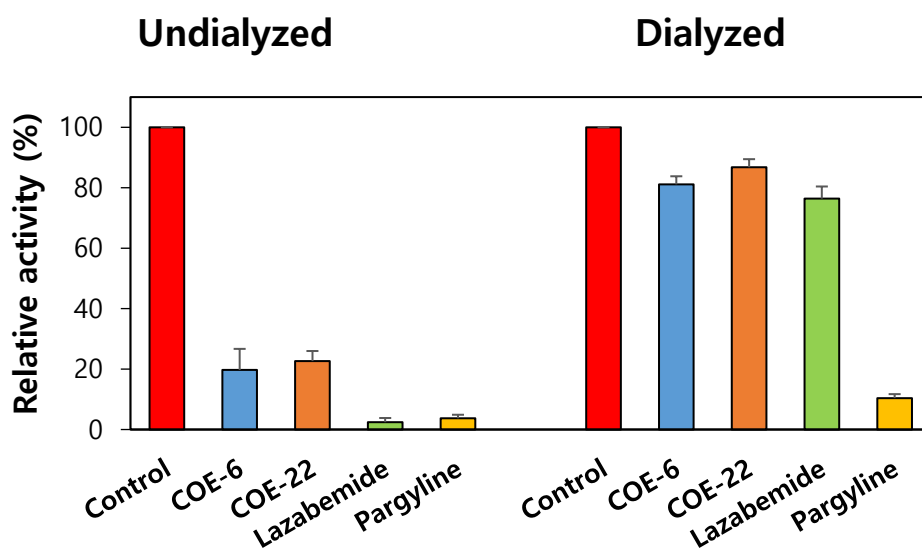
Figure 4. Recoveries of inhibitions of MAO-B by **COE-6** and **COE-22** as determined by dialysis.
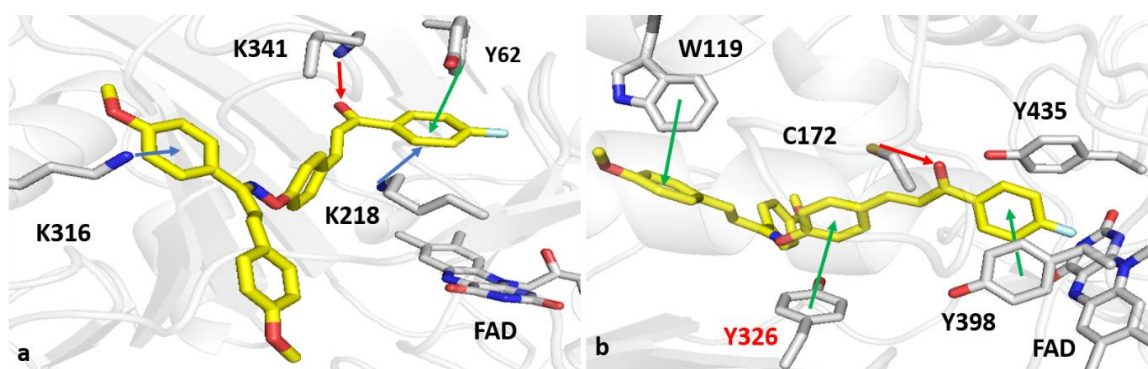
Figure 5. Top scored poses of **COE-22** in the binding sites of MAO-A (**a**) and MAO-B (**b**). Proteins are rendered as white cartoons, while ligands are rendered as yellow sticks. Green, blue and red arrows indicate $\pi-\pi$ interactions, cation-π interactions and hydrogen bonds, respectively. Y326, responsible for MAO-B selectivity, is labeled red.

Docking analysis did not report meaningful differences for interactions of **COE-6** towards MAO-A and MAO-B. The *para*-fluorine phenyl ring of **COE-6** is involved in $\pi-\pi$ interaction with Tyr407 of MAO-A, and it is trapped within an aromatic cage delimited by Tyr407, Tyr444, and FAD, unlike **COE-22**, as shown on panel (a) of Figure 6. When considering MAO-B, the *para*-fluorine phenyl ring of **COE-6** engages $\pi-\pi$ interaction with Tyr435 and faces the aromatic cage that is formed by Tyr435, Tyr398, and FAD. Notably, the selective MAO-B residue Tyr326 establishes $\pi-\pi$ interaction with the chalcone aromatic ring, and Cys172 makes a hydrogen bond with the carbonyl oxygen of the **COE-6** chalcone scaffold.

Docking studies carried out on **COE-6** and **COE-22** have proved that compound **COE-22** had the highest MAO-B affinity and appreciable selectivity. More specifically, **COE-22** interacts with MAO-A and MAO-B, but with different binding modes. In particular, in agreement with previous findings [24–29], the chalcone head of **COE-22** faces the FAD of MAO-B, whereas **COE-6** adopts similar poses for MAO-A and MAO-B, probably because of its smaller size. Interestingly, docking studies successfully explained at the molecular level the different experimental affinities of **COE-6** and **COE-22** for the two MAO isoforms. In particular, the gain in binding for MAO-B was mostly supported by the chance of forming $\pi-\pi$ hydrophobic interaction with Tyr326. This is a key residue, which changed

to I335 in MAO-A [49], capable of giving access to the binding pocket (for **COE-22** compound) and stabilizing the chalcone aromatic ring.
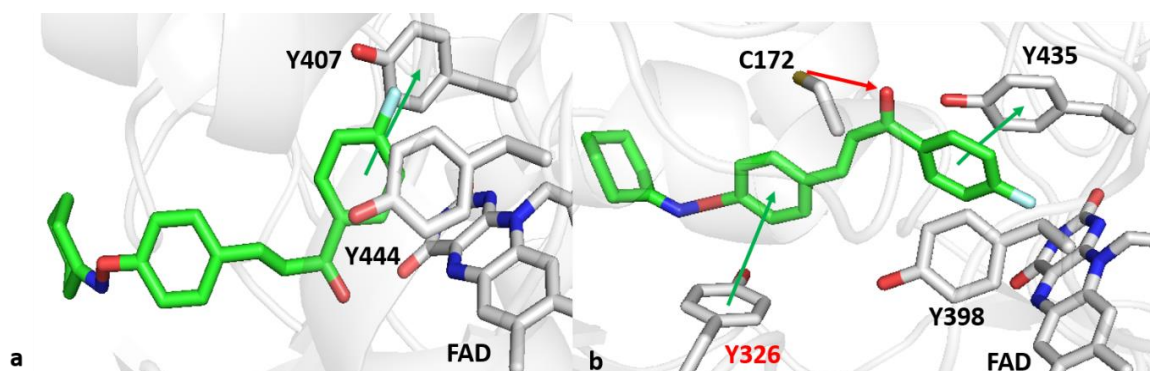

Figure 6. Top scored poses of **COE-6** in the binding sites of MAO-A (**a**) and MAO-B (**b**). Proteins and **COE-6** are depicted in white cartoons, and green sticks, respectively. Green arrows indicate $\pi-\pi$ interactions. MAO-B selective residue Y326 is highlighted in red.

3. Materials and Methods

3.1. Enzyme Assays

Recombinant hMAO-A and hMAO-B activities were assayed while using kynuramine (0.06 mM) and benzylamine (0.3 mM) as substrates, respectively, as described previously [50]. The substrate concentrations were $1.7 \times$ and $1.9 \times K_m$, respectively ($K_m = 0.036$ and 0.16 mM, respectively). AChE activity was measured using Type VI-S from *Electrophorus electricus* in the presence of 0.5 mM 5,5'-dithiobis(2-nitrobenzoic acid) and 0.5 mM acetylthiocholine iodide, as described previously [51,52]. Enzymes and chemicals were purchased from Sigma–Aldrich (St. Louis, MO, USA).

3.2. Analysis of Enzyme Inhibitions and Kinetics

The inhibitory activities of the 24 COEs synthesized against MAO-A and MAO-B were first investigated at a concentration of 1.0 μM, and IC_{50} values were then determined. AChE inhibitory activities were also determined, except at a concentration of 10 μM. Time-dependent inhibitions and reversibilities were measured, and kinetic studies were performed on the most potent MAO-B inhibitors, i.e., **COE-6**, and **COE-22**, as previously described [53]. Kinetic experiments were carried out at five substrate and three inhibitor concentrations.

3.3. Analysis of Inhibitor Reversibility

The reversibilities of compounds **COE-6**, and **COE-22** were analyzed while using a dialysis method after preincubating with MAO-B for 30 min, as previously described [54]. Reversibilities were determined for **COE-6**, **COE-22**, lazabemide (a reversible MAO-B reference inhibitor), and pargyline (an irreversible MAO-B reference inhibitor) at $\sim 2 \times IC_{50}$ concentrations, i.e., 0.004, 0.050, 0.080, and 0.040 μM, respectively. Relative activities of undialyzed (A_U) and dialyzed (A_D) samples were used to determine the reversibilities.

3.4. Computational Studies

The three-dimensional (3D) structures of MAO-A (PDB ID: 2Z5X) and MAO-B (PDB ID: 2V5Z) were obtained from the Protein Data Bank. The protein preparation wizard available in the Schrödinger suite was used to optimize X-ray crystal structures [55,56]. MAO-A and MAO-B active sites contained nine and eight water molecules, respectively. The LigPrep tool was used to optimize ligand structures and generate possible tautomers and ionization states at physiological pH. Docking simulations were

carried out using the QM polarized ligand docking protocol available from Schrödinger Suite. While retaining the rigidities of protein structures, QM polarized ligand docking allows for ligands with a certain degree of conformational flexibility. Centers of mass of X-ray cognate ligands of MAO-A and MAO-B structures were used as references for the cubic grid center.

The QM-polarized ligand docking protocol that was implemented in Glide was used with default options. This protocol uses three computational steps, that is: a) a standard precision (SP) initial docking using Glide; b) calculation of QM partial charges of the docked ligand based; and, c) a SP re-docking phase for each ligand pose when considering computed QM based charges.

A Molecular Mechanics/Generalized Born Surface Area (MM-GBSA) method was added to the workflow for the calculation of the binding free energies (ΔG) between protein and ligands in order to estimate ligand-binding affinities. Such a method is implemented in Prime available in the Schrodinger software 2018-2 (New York, NY, USA) [57]. Provided that ΔE_{MM} is the minimized energy of the ligand-protein complex, ΔG_{solv} is the solvation energy, and ΔG_{SA} is the binding energy of the surface area of compounds, with respect to MAO-A and MAO-B, ΔG_{bind} values were computed, as follows:

$$\Delta G_{bind} \ = \ \Delta E_{MM} + \Delta G_{solv} + \Delta G_{SA} \tag{1}$$

Obtained docking poses were minimized using Prime [57–59].

4. Conclusions

We evaluated the MAO-A, MAO-B, and AChE inhibitory activities of 24 previously synthesized chalcone oxime ethers (**COE-1–COE-24**). Most of the COEs exhibited significant and selective MAO-B inhibitory activity. Three compounds, viz., **COE-6**, **COE-7 (chalcone-ketoxime ethers),** and **COE-22 (chalcone-chalconeoxime ethers)**, potently inhibited MAO-B. However, only **COE-13** (**chalcone-ketoxime ethers**) significantly inhibited MAO-A and MAO-B. Notably, **COE-22** inhibited AChE well and potently inhibited MAO-B. Both lead MAO-B inhibitors, **COE-6 (chalcone-ketoxime ethers)** and **COE-22**, contained a F substitution, which once again supports the notion that fluorine inclusion can have a profound effect on the biological activity. Reversibility and kinetics studies on **COE-6** and **COE-22** showed that both potently, selectively, reversibly, and competitively inhibited MAO-B. We hope this preliminary study on these novel COEs encourages medicinal chemists to further explore MAO inhibition and conduct biological activity studies.

Conflicts of Interest: The authors declare no conflict of interest.

References

1. Querfurth, H.W.; LaFerla, F.M. Alzheimer's disease. *N. Engl. J. Med.* **2010**, *362*, 329–344. [CrossRef]
2. Mangialasche, F.; Solomon, A.; Winblad, B.; Mecocci, P.; Kivipelto, M. Alzheimer's disease: Clinical trials and drug development. *Lancet Neurol.* **2010**, *9*, 702–716. [CrossRef]
3. Zhang, H.-Y. One-compound-multiple-targets strategy to combat Alzheimer's disease. *FEBS Lett.* **2005**, *579*, 5260–5264. [CrossRef]
4. Youdim, M.B.H.; Buccafusco, J.J. Multi-functional drugs for various CNS targets in the treatment of neurodegenerative disorders. *Trends Pharmacol. Sci.* **2005**, *26*, 27–35. [CrossRef]
5. Mathew, B.; Parambi, D.G.T.; Mathew, G.E.; Uddin, M.S.; Inasu, S.T.; Kim, H.; Marathakam, A.; Unnikrishnan, M.K.; Carradori, S. Emerging therapeutic potentials of dual-acting MAO and AChE inhibitors in Alzheimer's and Parkinson's diseases. *Arch. Pharm. Chem. Life Sci.* **2019**, *352*, e1900177. [CrossRef]

6. Bolognesi, M.L.; Matera, R.; Minarini, A.; Rosini, M.; Melchiorre, C. Alzheimer's disease new approaches to drug discovery. *Curr. Opin. Chem. Biol.* **2009**, *13*, 303–308. [CrossRef]

7. Bolognesi, M.L.; Cavalli, A.; Valgimigli, L.L.; Bartolini, M.; Rosini, M.; Andrisano, V.; Recanatini, M.; Melchiorre, C. Multi-target-directed drug design strategy: From a dual binding site acetylcholinesterase inhibitor to a trifunctional compound against Alzheimer's disease. *J. Med. Chem.* **2007**, *50*, 6446–6449. [CrossRef]

8. Youdim, M.B.H.; Edmondson, D.; Tipton, K.F. The therapeutic potential of monoamine oxidase inhibitors. *Nat. Rev. Neurosci.* **2006**, *7*, 295–309. [CrossRef]

9. Youdim, M.B.H.; Maruyama, W.; Naoi, M. Neuropharmacological, neuroprotective and amyloid precursor processing properties of selective MAO-B inhibitor antiparkinsonian drug, rasagiline. *Drugs Today* **2005**, *41*, 369–391. [CrossRef]

10. Cavalli, A.; Bolognesi, M.L.; Capsoni, S.; Andrisano, V.; Bartolini, M.; Margotti, E.; Cattaneo, A.; Recanatini, M.; Melchiorre, C. A small molecule targeting the multifactorial nature of Alzheimer's disease. *Angew. Chem. Int.* **2007**, *46*, 3689–3692. [CrossRef]

11. Van der Schyf, C.J.; Geldenhuys, W.J.; Youdim, M.B.H. Multifunctional drugs with different CNS targets for neuropsychiatric disorders. *J. Neurochem.* **2006**, *99*, 1033–1048. [CrossRef] [PubMed]

12. Dimmock, J.R.; Elias, D.W.; Beazely, M.A.; Kandepu, N.M. Bioactivities of chalcones. *Curr. Med. Chem.* **1999**, *6*, 1125–1149. [PubMed]

13. Mathew, B.; Suresh, J.; Anbazhagan, S.; Paulraj, J.; Krishnan, G.K. Heteroaryl chalcones: Mini review about their therapeutic voyage. *BioMed. Prev. Nutr.* **2014**, *4*, 451–458. [CrossRef]

14. Jandial, D.D.; Blair, C.A.; Zhang, S.; Krill, L.S.; Zhang, Y.B.; Zi, X. Molecular targeted approaches to cancer therapy and prevention using chalcones. *Curr. Cancer Drug Targets* **2014**, *14*, 181–200. [CrossRef]

15. Singh, P.; Anand, A.; Kumar, V. Recent developments in biological activities of chalcones: A mini review. *Eur. J. Med. Chem.* **2014**, *85*, 758–777. [CrossRef]

16. Mahapatra, D.K.; Bharti, S.K.; Asati, V. Chalcone scaffold as anti-infective agents: Structural and molecular target perspectives. *Eur. J. Med. Chem.* **2015**, *101*, 496–524. [CrossRef]

17. Mathew, B.; Haridas, A.; Suresh, J.; Mathew, G.E.; Ucar, G.; Jayaprakash, V. Monoamine oxidase inhibitory actions of chalcones: A mini review. *Cent. Nerv. Syst. Agents Med. Chem.* **2016**, *16*, 120–136. [CrossRef]

18. Chimenti, F.; Fioravanti, R.; Bolasco, A.; Chimenti, P.; Secci, D.; Rossi, F.; Yáñez, M.; Orallo, F.; Ortuso, F.; Alcaro, S. Chalcones: A valid scaffold for monoamine oxidases inhibitors. *J. Med. Chem.* **2009**, *52*, 2818–2824. [CrossRef]

19. Robinson, S.J.; Petzer, J.P.; Petzer, A.; Bergh, J.J.; Lourens, A.C.U. Selected furanochalcone as inhibitors of monoamine oxidase. *Bioorg. Med. Chem. Lett.* **2013**, *23*, 4985–4989. [CrossRef]

20. Jo, G.; Ahn, S.; Kim, B.G.; Park, H.R.; Kim, Y.H.; Cho, A.H.; Koh, D.; Chong, Y.; Ahn, H.; Lim, Y. Chromenyl chalcones with inhibitory effects on monoamine oxidase B. *Bioorg. Med. Chem.* **2013**, *21*, 7890–7897. [CrossRef]

21. Morales-Camilo, N.; Salas, C.O.; Sanhueza, C.; Espinosa-Bustos, C.; Sepulveda-Boza, S.; Reyes-Parada, M.; Gonzalez-Nilo, F.; Caroli-Rezende, M.; Fierro, A. Synthesis, biological evaluation, and molecular simulation of chalcones and aurones as selective MAO-B inhibitors. *Chem. Biol. Drug Des.* **2015**, *85*, 685–695. [CrossRef] [PubMed]

22. Choi, J.W.; Jang, B.K.; Cho, N.; Park, J.H.; Yeon, S.K.; Ju, E.J.; Lee, Y.S.; Han, G.; Pae, A.M.; Kim, D.J.; et al. Synthesis of a series of unsaturated ketone derivatives as selective and reversible monoamine oxidase inhibitors. *Bioorg. Med. Chem.* **2015**, *23*, 6486–6496. [CrossRef] [PubMed]

23. Mathew, B. Unraveling the structural requirements of chalcone chemistry towards monoamine oxidase inhibition. *Cent. Nerv. Syst. Agents Med. Chem.* **2019**, *19*, 6–7. [CrossRef] [PubMed]

24. Mathew, B.; Mathew, G.E.; Uçar, G.; Baysal, I.; Suresh, J.; Vilapurathu, J.K.; Prakasan, A.; Suresh, J.K.; Thomas, A. Development of fluorinated methoxylated chalcones as selective monoamine oxidase-B inhibitors: Synthesis, biochemistry and molecular docking studies. *Bioorg. Chem.* **2015**, *62*, 22–29. [CrossRef] [PubMed]

25. Mathew, B.; Uçar, G.; Yabanoğlu-Çiftçi, S.; Baysal, I.; Suresh, J.; Mathew, G.E.; Vilapurathu, J.K.; Nadeena, A.M.; Nabeela, P.; Lakshmi, V.; et al. Development of fluorinated thienylchalcones as monoamine oxidase-b inhibitors: Design, synthesis, biological evaluation and molecular docking studies. *Lett. Org. Chem.* **2015**, *12*, 605–613. [CrossRef]

26. Mathew, B.; Mathew, G.E.; Uçar, G.; Baysal, I.; Suresh, J.; Mathew, S. Potent and selective monoamine oxidase-b inhibitory activity: Fluoro- vs trifluoromethyl-4-hydroxylated chalcone derivatives. *Chem. Biodivers.* **2016**, *13*, 1046–1052. [CrossRef]

27. Mathew, B.; Haridas, A.; Uçar, G.; Baysal, I.; Adeniyi, A.A.; Soliman, M.E.S.; Joy, M.; Mathew, G.E.; Lakshmanan, B.; Jayaprakash, V. Exploration of chlorinated thienyl chalcones: A new class of monoamine oxidase-B inhibitors. *Int. J. Biol. Macromol.* **2016**, *91*, 680–695. [CrossRef]

28. Mathew, B.; Haridas, A.; Uçar, G.; Baysal, I.; Joy, M.; Mathew, G.E.; Lakshmanan, B.; Jayaprakash, V. Synthesis, biochemistry, and computational studies of brominated thienyl chalcones: A new class of reversible MAO-B inhibitors. *ChemMedChem* **2016**, *11*, 1161–1171. [CrossRef]

29. Mathew, B.; Uçar, G.; Mathew, G.E.; Mathew, S.; Purapurath, P.K.; Moolayil, F.; Mohan, S.; Varghese Gupta, S. Monoamine oxidase inhibitory activity: Methyl- versus chloro-chalcone derivatives. *ChemMedChem* **2016**, *11*, 2649–2655. [CrossRef]

30. Sasidharan, R.; Manju, S.L.; Uçar, G.; Baysal, I.; Mathew, B. Identification of indole based chalcones: Discovery of potent, selective and reversible class of MAO-B inhibitors. *Arch. Pharm. Chem. Life Sci.* **2016**, *349*, 627–637. [CrossRef]

31. Mathew, B.; Uçar, G.; Raphael, C.; Mathew, G.E.; Joy, M.; Machaba, K.E. Characterization of thienylchalcones as hMAO-B inhibitors: Synthesis, biochemistry and molecular dynamics studies. *ChemistrySelect* **2017**, *2*, 11113–11119. [CrossRef]

32. Sasidharan, R.; Baek, S.C.; Manju, S.L.; Kim, H.; Mathew, B. Imidazole bearing chalcones as new class of monoamine oxidase inhibitors. *Biomed. Pharmacother.* **2018**, *106*, 8–13. [CrossRef] [PubMed]

33. Suresh, J.; Baek, S.C.; Ramakrishnan, S.P.; Kim, H.; Mathew, B. Discovery of potent and reversible MAO-B inhibitors as furanochalcones. *Int. J. Biol. Macromol.* **2018**, *108*, 660–664. [CrossRef]

34. Mathew, B.; Baek, S.C.; Parambi, D.G.T.; Lee, J.P.; Mathew, G.E.; Jayanthi, S.; Devaraji, D.; Raphael, C.; Vinod, D.; Kondarath, S.S.; et al. Potent and highly selective dual-targeting monoamine oxidase-B inhibitors: Fluorinated chalcones of morpholine versus imidazole. *Arch. Pharm. Chem. Life Sci.* **2019**, *352*, e1800309. [CrossRef]

35. Shalaby, R.; Petzer, J.P.; Petzer, A.; Aahraf, U.M.; Atari, E.; Alasmari, F.; Kumarasamy, S.; Sari, Y.; Khali, A. SAR and molecular mechanism studies of monoamine oxidase inhibition by selected chalcone analogs. *J. Enzym. Inhib. Med. Chem.* **2019**, *34*, 863–876. [CrossRef]

36. Lakshminarayan, B.; Baek, S.C.; Kannappan, N.; Mangiatordi, G.F.; Nicolotti, O.; Subburaju, T.; Kim, H.; Mathew, B. Ethoxylated head of chalcones as a new class of multi-targeted MAO inhibitors. *ChemistrySelect* **2019**, *4*, 6614–6619. [CrossRef]

37. Reeta Baek, S.C.; Lee, J.P.; Rangarajan, T.M.; Ayushee; Singh, R.P.; Singh, M.; Mangiatordi, G.F.; Nicolotti, O.; Kim, H.; Mathew, B. Ethyl acetohydroxamate incorporated chalcones: Unveiling a novel class of chalcones for multitarget monoamine oxidase-B inhibitors against Alzheimer's disease. *CNS Neurol. Disord. Drug Targets* **2019**, *8*, 643–654.

38. Johnson, S.M.; Petrassi, H.M.; Palaninathan, S.K.; Mohamedmohaideen, N.N.; Purkey, H.E.; Nichols, C.; Chiang, K.P.; Walkup, T.; Sacchettini, J.C.; Sharpless, K.B.; et al. Bisaryloxime ethers as potent inhibitors of transthyretin amyloid fibril formation. *J. Med. Chem.* **2005**, *48*, 1576–1587. [CrossRef]

39. Tsuchiya, K.; Kondo, M.; Kida, M.; Nakao, M.; Iwahi, T.; Nishi, T.; Noji, Y.; Takeuchi, M.; Nozaki, Y. Cefmenoxime (SCE-1365), a novel broad-spectrum cephalosporin: In vitro and in vivo antibacterial activities. *Antimicrob. Agents Chemother.* **1981**, *19*, 56–65. [CrossRef]

40. Shibl, A.M.; Ishag, A.H.; Durgham, S.M. Comparative *in vitro* antibacterial activity of aztreonam against clinical isolates of gram-negative bacteria. *Chemotheraphy* **1989**, *35*, 72–76. [CrossRef]

41. Bryskier, A. Roxithromycin: Review of its antimicrobial activity. *J. Antimicrob. Chemother.* **1998**, *41*, 1–21. [CrossRef] [PubMed]

42. Carty, E.; Macey, M.; Mccartney, S.A.; Rampton, D.S. Ridogrel, a dual thromboxane synthase inhibitor and receptor antagonist: Anti-inflammatory profile in inflammatory bowel disease. *Aliment. Pharmacol. Ther.* **2000**, *14*, 807–817. [CrossRef] [PubMed]

43. van Hoogdalem, E.J.; van den Hoven, W.E.; Terpstra, I.J.; van Zijtveld, J.; Verschoor, J.S.C.; Visser, J.N. Nail penetration of the antifungal agent oxiconazole after repeated topical application in healthy volunteers, and the effect of acetylcysteine. *Eur. J. Pharm. Sci.* **1997**, *5*, 119–127. [CrossRef]

44. Strupczewski, J.T.; Allen, R.C.; Gardner, B.A.; Schmid, B.L.; Stache, U.; Glamkowski, E.J.; Jones, M.C.; Ellis, D.B.; Huger, F.P.; Dunn, R.W. Synthesis and neuroleptic activity of 3-(1-substituted-4-piperidinyl)-1,2-benzisoxazoles. *J. Med. Chem.* **1985**, *28*, 761–769. [CrossRef] [PubMed]

45. Reeta Rajendran, V.; Rangarajan, T.M.; Ayushee; Singh, R.P.; Singh, M. Synthesis of novel chalcones through palladium-catalyzed C–O cross-coupling reaction of bromo-chalcones with ethyl acetohydroxamate and their antiplasmodial evaluation against *Plasmodium falcipuram* in vitro. *Bioorg. Chem.* **2019**, *86*, 631–640. [CrossRef]

46. Reeta Rangarajan, T.M.; Kaushik, K.; Singh, R.P.; Singh, M.; Singh, R.P. Efficient solvent- and temperature-tuned access to aldoxime ethers and phenolic functions by Pd-catalyzed C–O cross-coupling of aldoximes with aryl bromides and bromo-chalcones. *New J. Chem.* **2020**, *44*, 1326–1336. [CrossRef]

47. Reeta Rangarajan, T.M.; Singh, R.P.; Singh, M. An easy access to oxime ethers by Pd-catalyzed C–O cross-coupling of activated aryl bromides with ketoximes and chalcone oximes. *Chin. J. Chem.* **2020**, *38*, 830–836.

48. Mathew, B.; Carradori, S.; Guglielmi, P.; Uddin, M.S.; Kim, H. New aspects of monoamine oxidase-B inhibitors. The key role of halogens to open the golden door. *Curr. Med. Chem.* **2020**, *27*, 1–17. [CrossRef]

49. Mangiatordi, G.F.; Alberga, D.; Pisani, L.; Gadaleta, D.; Trisciuzzi, D.; Farina, R.; Carotti, A.; Lattanzi, G.; Catto, M.; Nicolotti, O. A rational approach to elucidate human monoamine oxidase molecular selectivity. *Eur. J. Pharm. Sci.* **2017**, *101*, 90–99. [CrossRef]

50. Mathew, B.; Baek, S.C.; Parambi, D.G.T.; Lee, J.P.; Joy, M.; Rilda, P.R.A.; Randev, R.V.; Nithyamol, P.; Vijayan, V.; Inasu, S.T.; et al. Selected aryl thiosemicarbazones as a new class of multi-targeted monoamine oxidase inhibitors. *MedChemComm* **2018**, *9*, 1871–1881. [CrossRef]

51. Lee, H.W.; Ryu, H.W.; Kang, M.G.; Park, D.; Oh, S.R.; Kim, H. Potent selective monoamine oxidase B inhibition by maackiain, a pterocarpan from the roots of *Sophora flavescens*. *Bioorg. Med. Chem. Lett.* **2016**, *26*, 4714–4719. [CrossRef] [PubMed]

52. Baek, S.C.; Lee, H.W.; Ryu, H.W.; Kang, M.G.; Park, D.; Kim, S.H.; Cho, M.L.; Oh, S.R.; Kim, H. Selective inhibition of monoamine oxidase A by hispidol. *Bioorg. Med. Chem. Lett.* **2018**, *15*, 584–588. [CrossRef] [PubMed]

53. Ellman, G.L.; Courtney, K.D.; Andres, V.; Feather-Stone, R.M., Jr. A new and rapid colorimetric determination of acetylcholinesterase activity. *Biochem. Pharmacol.* **1961**, *7*, 88–95. [CrossRef]

54. Baek, S.C.; Park, M.H.; Ryu, H.W.; Lee, J.P.; Kang, M.G.; Park, D.; Park, C.M.; Oh, S.R.; Kim, H. Rhamnocitrin isolated from *Prunus padus* var. *seoulensis*: A potent and selective reversible inhibitor of human monoamine oxidase A. *Bioorg. Chem.* **2018**, *28*, 317–325. [CrossRef] [PubMed]

55. Son, S.Y.; Ma, J.; Kondou, Y.; Yoshimura, M.; Yamashita, E.; Tsukihara, T. Structure of human monoamine oxidase A at 2.2-A resolution: The control of opening the entry for substrates/inhibitors. *Proc. Natl. Acad. Sci. USA* **2008**, *105*, 5739–5744. [CrossRef] [PubMed]

56. Binda, C.; Wang, J.; Pisani, L.; Caccia, C.; Carotti, A.; Salvati, P.; Edmondson, D.E.; Mattevi, A. Structures of human monoamine oxidase B complexes with selective non-covalent inhibitors: Safinamide and coumarin analogs. *J. Med. Chem.* **2007**, *50*, 5848–5852. [CrossRef]

57. *Schrödinger Release 2018-2, Prime*; Schrödinger, LLC: New York, NY, USA, 2018.

58. *Schrödinger Release 2018-2: Glide*; Schrödinger, LLC: New York, NY, USA, 2018.

59. Genheden, S.; Ryde, U. The MM/PBSA and MM/GBSA methods to estimate ligand-binding affinities. *Expert Opin. Drug Discov.* **2015**, *10*, 449–461. [CrossRef]

Sample Availability: Samples of the compounds are available from the authors.